

OPEN SET FACE FORGERY DETECTION VIA DUAL-LEVEL EVIDENCE COLLECTION

005 **Anonymous authors**

006 Paper under double-blind review

ABSTRACT

011 The proliferation of face forgeries has increasingly undermined confidence in the
 012 authenticity of online content. Given the rapid development of face forgery gen-
 013 eration algorithms, new fake categories are likely to keep appearing, posing a
 014 major challenge to existing face forgery detection methods. Despite recent ad-
 015 vances in face forgery detection, existing methods are typically limited to binary
 016 Real-vs-Fake classification or the identification of known fake categories, and are
 017 incapable of detecting the emergence of novel types of forgeries. In this work,
 018 we study the *Open Set Face Forgery Detection (OSFFD)* problem, which de-
 019 demands that the detection model recognize novel fake categories. We reformu-
 020 late the OSFFD problem and address it through uncertainty estimation, enhancing
 021 its applicability to real-world scenarios. Specifically, we propose the Dual-Level
 022 Evidential face forgery Detection (DLED) approach, which collects and fuses
 023 category-specific evidence on the spatial and frequency levels to estimate pre-
 024 diction uncertainty. Extensive evaluations conducted across diverse experimen-
 025 tal settings demonstrate that the proposed DLED method achieves state-of-the-art
 026 performance, outperforming various baseline models by an average of 20% in
 027 detecting forgeries from novel fake categories. Moreover, on the traditional Real-
 028 versus-Fake face forgery detection task, our DLED method concurrently exhibits
 029 competitive performance.

1 INTRODUCTION

033 Deepfakes, which use deep learning techniques to generate or modify faces and voices, continue to
 034 rapidly increase in both sophistication and accessibility. The diversity of deepfake forgeries (Kor-
 035 shunova et al., 2017; Karras, 2017; Shen & Liu, 2017; Siarohin et al., 2019) causes different visual
 036 artifacts to appear in the generated deepfakes, making deepfake detection increasingly difficult. Ac-
 037 cording to a survey by Mirsky et al. (Mirsky & Lee, 2021), existing face deepfake forgeries can
 038 generally be organized into four categories: Face Swapping (FS), Face Reenactment (FR), Entire
 039 Face Synthesis (EFS), and Face Editing (FE). As new generation methods continue to emerge, it is
 040 likely that novel categories of facial deepfakes will be developed.

041 Despite progress in deepfake detection under closed set scenarios (Yan et al., 2023b; Qian et al.,
 042 2020; Gu et al., 2022; Ni et al., 2022), where both training and testing data contain the same known
 043 fake forgeries¹, these methods have yet to fully address the challenge of generalizing to unseen fake
 044 forgeries. Some studies (Wang et al., 2020; Cao et al., 2022; Nadimpalli & Rattani, 2022; Zhuang
 045 et al., 2022; Sun et al., 2023) have proposed mechanisms to improve generalization to unseen for-
 046 geries. However, their overall performance remains suboptimal, and they fail to detect the emergence
 047 of novel fake categories.

048 In this paper, we study the Open Set Face Forgery Detection (OSFFD) problem to address this
 049 issue. OSFFD was proposed in (Diniz & Rocha, 2024; Zhou et al., 2024), but it remains an under-
 050 explored problem. Traditional deepfake detection and attribution tasks either distinguish between
 051 real and fake images or assign forgeries to predefined categories. In contrast, OSFFD determines

052 ¹In this paper, we define “fake forgeries” as specific deepfake methodologies, and “fake categories” as the
 053 broader groups to which these methodologies belong; e.g., FSGAN (Nirkin et al., 2019) is the fake forgery and
 Face Swapping is its according fake category.

whether a given face belongs to a novel fake category, while simultaneously performing multiclass classification among real and known fake categories. The difference among these settings is shown in Figure 1. The aforementioned studies approached the OSFFD problem by training models on labeled data for seen classes (real and known fake categories), and unlabeled data for novel fake categories. This setup has practical limitations as data from a novel fake category would not be integrated into datasets immediately after its proliferation. In this paper, we reformulate the OSFFD problem by restricting model training to only real and known fake categories, which enhances the real-world applicability of OSFFD.

To address the OSFFD problem, we formulate it as an uncertainty estimation issue that assesses the confidence of model predictions based on the evidence collected from the data. During training, the model is exposed to known fake categories and learns to assign low uncertainty to these samples. At test time, samples from unknown categories are expected to yield high uncertainty scores, facilitating their detection.

In this paper, we propose a novel *Dual-Level Evidential face forgery Detection* approach, DLED, that simultaneously identifies emerging, unknown fake categories and performs multiclass classification among real and known fake categories. To enable novel category recognition, DLED leverages Evidential Deep Learning (EDL) (Senoy et al., 2018; 2020; Shi et al., 2020) for classification and uncertainty estimation. However, unlike conventional open set classification, OSFFD operates on structured facial imagery whose spatial semantic patterns alone are insufficiently discriminative (Wang et al., 2020). Accordingly, DLED augments these cues with complementary low-level frequency artifacts, yielding a more effective application of EDL. Because both sources are informative, detection decisions should reflect their joint support. To this end, we introduce an uncertainty-guided evidence fusion mechanism grounded in Dempster’s combination rule (Senz & Ferson, 2002), enabling DLED to integrate evidence on both the spatial and frequency levels into a unified, comprehensive uncertainty estimate. Furthermore, we propose an improved uncertainty estimation approach to enhance the model’s capability to detect novel fake, as the original EDL formulation can be affected by evidence from irrelevant classes, resulting in suboptimal uncertainty quantification.

Compared with existing face forgery detection methods, a key advantage of our DLED model lies in its ability to promptly detect newly emerging fake categories and avoid misclassification, without relying on any prior knowledge of these categories. While existing deepfake detection algorithms can be adapted to be feasible in the OSFFD problem, e.g., one-class detectors (Shiohara & Yamasaki, 2022; Khalid & Woo, 2020; Larue et al., 2023) can combine with a separate multiclass classifier, they often struggle to balance between accurate novel category detection and effective multiclass classification. In addition, our methodology is grounded in principled reasoning, offering clear interpretability for the OSFFD results.

In summary, our contribution is three-fold:

- We reformulate the Open Set Face Forgery Detection (OSFFD) problem, eliminating the reliance on unlabeled data from novel fake categories during model training, making it more applicable in real life.
- We propose leveraging EDL to treat the OSFFD as an uncertainty estimation problem, enabling the model to determine whether a face image originates from a novel fake category.
- We propose the DLED approach, which aggregates and fuses evidence on both the spatial and frequency levels to estimate prediction uncertainty. Extensive empirical results validate its effectiveness and demonstrate its superiority over various baseline models.

2 RELATED WORK

Deepfake Detection. A wide range of deepfake detection approaches have been studied in the literature (Huang et al., 2022). Most existing methods (Sun et al., 2022; Ni et al., 2022; Zhuang

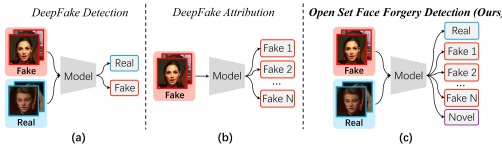


Figure 1: **Comparison with existing settings.** Different from DeepFake Detection (a) and Attribution (b), Open Set Face Forgery Detection (c) aims to identify whether a forgery originates from a novel fake category or not while simultaneously performing multiclass classification among real and known fake categories.

108 et al., 2022; Cao et al., 2022) leverage spatial patterns to detect manipulation artifacts, while others (Luo et al., 2021; Gu et al., 2022; Zhang et al., 2019) exploit discrepancies in the frequency
 109 domain to reveal forgery traces. Some studies also (Tan et al., 2024; Wang et al., 2023b; Guillaro
 110 et al., 2023) integrated features from complementary modalities, such as noise patterns, to further
 111 distinguish fake faces. One-class anomaly detection methods (Khalid & Woo, 2020; Shiohara &
 112 Yamasaki, 2022; Larue et al., 2023) treat real faces as the positive class and all other data as anomalous
 113 outliers, training the model exclusively on the positive class to distinguish between real and
 114 fake faces. Recent works (Ojha et al., 2023; Khan & Dang-Nguyen, 2024) find that the pretrained
 115 CLIP (Radford et al., 2021) model performs well on unseen forgeries. Based on this finding, several
 116 recent works (Liu et al., 2024b;a; Yang et al., 2025) designed diverse adaptations for CLIP to en-
 117 hance its detection capabilities. However, these approaches are limited by their exclusive focus on
 118 Real-vs-Fake classification, which overlooks the differences among different fake categories.
 119

120 **Deepfake Attribution.** The deepfake attribution task aims to identify the source of fake faces so
 121 that models can provide persuasive explanations for the results of deepfake detection. However,
 122 most of these methods (Wu et al., 2024; Huang et al., 2023; Yang et al., 2022; Zhong et al., 2023)
 123 are limited to the closed set scenario. Few methods have utilized the “open world” setting to track
 124 unseen forgeries. The open-world GAN (Girish et al., 2021) method is designed to detect images
 125 generated by previously unseen GANs, but its framework does not extend to other manipulations
 126 such as face editing. Another work, CPL (Sun et al., 2023), introduced a benchmark which encom-
 127 passes a broader array of unseen forgeries derived from multiple known categories. However, this
 128 setting relies on access to unlabeled data from such forgeries during training and does not determine
 129 whether a given forgery originates from a novel category, thereby limiting its practical applicability.
 130 Although recent works (Wang et al., 2024a; 2023a) introduced open set classification for forgeries,
 131 their settings do not differentiate between unseen forgeries originating from known categories and
 132 those from entirely novel categories, nor can they determine whether a face is real or fake.
 133

134 **Open Set Recognition.** Open Set Recognition is a well-defined task that recognizes known classes
 135 and differentiates the unknown. The pioneering work (Scheirer et al., 2012) formalized the definition
 136 and introduced a “one-vs-set” machine based on binary SVM. Prototype learning and metric learning
 137 methods (Chen et al., 2021; Yang et al., 2020; Zhang & Ding, 2021) have been applied to identify
 138 the unknown by keeping unknown samples at large distances to prototypes of known class data.
 139 Recently, uncertainty estimation methods (Wang et al., 2021; Bao et al., 2021; Fan et al., 2024;
 140 2023) using Evidential Deep Learning (EDL) have shown promising results on open set recognition
 141 problems. EDL (Sensoy et al., 2018; 2020; Shi et al., 2020) works well to quantify model confidence
 142 and prediction uncertainty, exhibiting high efficacy in handling unseen data types, and it has been
 143 further broadened to encompass multi-view classification (Han et al., 2020; Huang et al., 2024). To
 144 the best of our knowledge, this paper is the first to integrate EDL into the OSFFD problem.
 145

3 OPEN SET FACE FORGERY DETECTION

Definition.

146 As depicted in Figure 2, Open Set Face Forgery
 147 Detection (OSFFD) addresses a practical problem:
 148 leveraging knowledge from seen classes (i.e., real
 149 faces and faces from known fake categories) to clas-
 150 sify a given face as either belonging to a seen class or
 151 to the newly emerging, unseen fake category. In the
 152 training phase, the model is exposed exclusively to
 153 images from seen classes, while images from novel
 154 fake categories are reserved for testing purposes.
 155

156 **Motivation.** OSFFD requires a model to sim-
 157 taneously discover novel fake categories and per-
 158 form multiclass classification. Among these two ob-
 159 jectives, novel fake category discovery is the core
 160 challenge. However, most existing detectors (Ojha
 161 et al., 2023; Yan et al., 2024a) emphasize out-of-
 162 distribution (OOD) generalization, which target binary real-vs-fake discrimination on unseen testing



163 **Figure 2: Illustration for Fake Categories in**
 164 **OSFFD.** Real faces and fake faces from the seen
 165 categories are used to train the model. Subse-
 166 quently, the model is evaluated on test data that
 167 includes both seen classes and previously unseen
 168 categories. In the figure, the labels EFS, FR, and
 169 FS denote seen categories, whereas FE represents
 170 an unseen category.

samples. As a result, they neither support multiclass classification nor distinguish novel fake categories, rendering them unsuitable for OSFFD. One alternative is a two-stage pipeline that first partitions samples into seen versus unseen class via OOD detection (Khalid & Woo, 2020; Shiohara & Yamasaki, 2022) and then applies a face-forgery classifier to seen classes; but this decoupled design optimizes different training objectives across stages and offers limited theoretical interpretability. Additionally, existing open set recognition (OSR) methods (Zhang & Xiang, 2023; Lang et al., 2024) could hardly perform well when directly applied to OSFFD as the data in OSFFD consist of highly structured facial imagery that requires additional mechanisms to extract discriminative representations. Therefore, novel algorithms need to be developed to address the OSFFD problem.

Formulation. Given a labeled training set $D_S = \{(x_i, y_i)\}_{i=1}^M$ consisting of M labeled samples from K seen classes comprising the Real class and N known fake categories (i.e., $K = N + 1$, $y_i \in \{1, \dots, K\}$) and a test set D_T containing samples from the face class set $\{R, F_1, \dots, F_N, F_{N+1}, \dots, F_{N+U}\}$, where U is the number of unknown fake categories, we denote the embedding space of class $k \in [1, K]$ as P_k , and its corresponding open space as O_k . The open space is further divided into two subspaces: the positive open space from other known classes O_k^{pos} and the negative open space O_k^{neg} that represents the remaining infinite unknown region.

For a single class k , the samples $D_S^k \in P_k$, $D_S^{\neq k} \in O_k^{\text{pos}}$, and $D_V \in O_k^{\text{neg}}$ are positive training data, negative training data and potential unknown data respectively. Then, we could use a simple binary classification model $\Psi_k(x) \rightarrow \{0, 1\}$ to detect unseen classes (Chen et al., 2021) and optimize the model by minimizing the expected risk R^k :

$$\arg \min_{\Psi_k} R^k = R_c(\Psi_k, P_k \cup O_k^{\text{pos}}) + \alpha \cdot R_o(\Psi_k, O_k^{\text{neg}}), \quad (1)$$

where α is a positive constant, R_c is the empirical classification risk on the known data, and R_o is the open space risk (Scheirer et al., 2012). R_o measures the likelihood of labeling unknown samples as either known or unknown classes, expressed as a nonzero integral function over the space O_k^{neg} :

$$R_o(\Psi_k, O_k^{\text{neg}}) = \frac{\int_{O_k^{\text{neg}}} \Psi_k(x) dx}{\int_{P_k \cup O_k} \Psi_k(x) dx}. \quad (2)$$

The more frequently the negative open space O_k^{neg} is labeled as positive, the higher the associated open space risk.

We extend single-class detection to the multiclass OSFFD setting by integrating multiple binary classification models Ψ_k using a one-vs-rest strategy. With Eq. 1, the overall expected risk is computed as the sum over all seen classes: $\sum_{k=1}^K R^k$. This is equivalent to training a multiclass classification model $\mathcal{F} = \odot(\Psi_1, \dots, \Psi_K)$ for K -class classification, where $\odot(\cdot)$ denotes the integration operation. The overall training optimization objective is formulated as:

$$\arg \min \{R_c(\mathcal{F}, D_S) + \alpha \cdot \sum_{k=1}^K R_o(\mathcal{F}, D_V)\}, \quad (3)$$

which demands the model to minimize the combination of the classification risk on seen classes and the open space risk on unseen classes. Therefore, our goal is to train a multiclass classification model $\mathcal{F}(\cdot)$, parameterized by θ , on K seen classes to accurately classify faces as either real or belonging to one of the known fake categories, while simultaneously detecting novel fake categories as a distinct $(K + 1)^{\text{th}}$ class. We further formulate OSFFD as an uncertainty estimation problem: the model $\mathcal{F} : \mathcal{X} \rightarrow (\tilde{y}, \tilde{u})$ outputs a predicted category label $\tilde{y} \in \{1, \dots, K\}$ and its associated predictive uncertainty \tilde{u} . If the predictive uncertainty exceeds the class-specific threshold $\tau_{\tilde{y}}$, i.e., $\tilde{u} > \tau_{\tilde{y}}$, the predicted label is deemed unreliable and the instance is assigned to the novel fake category.

4 METHODOLOGY

To solve the formulated uncertainty estimation problem, we utilize established techniques such as MaxLogit and Evidential Deep Learning.

Plug-in OSR Techniques. Maximum Softmax Probability (Hendrycks et al., 2019) and MaxLogit (Wang et al., 2022) detectors are two widely used plug-in OSR techniques, which utilize the maximum Softmax probabilities and the maximum logits as the model prediction confidence with no extra computational costs.

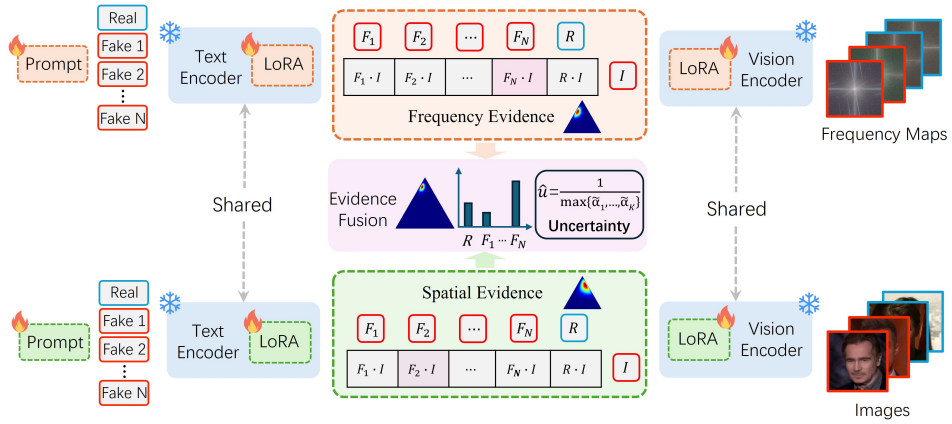


Figure 3: **Overview of DLED.** DLED collects and fuses evidence from both the spatial and frequency domains to estimate prediction uncertainty. Our improved uncertainty estimation \hat{u} is applied to achieve better detection performance. F_N represents the N -th fake category and K is the total known class number. If the uncertainty for the given sample is larger than the computed threshold, its label will be reassigned to the novel fake category. In the evidence illustration, we present a demonstration of a three-class classification scenario ($K = 3$).

Evidential Deep Learning. Evidential Deep Learning (EDL) is an effective technique that performs multiclass classification and uncertainty modeling by introducing the framework of Dempster-Shafer Theory (Senz & Ferson, 2002) and subjective logic (Jøsang, 2016). For a K -class classification problem, given a sample x and a model \mathcal{F} parameterized by θ , the predicted evidence is given by $e = h(\mathcal{F}(x; \theta)) \in R^K$, where h is an evidence function. With total strength $S = \sum_{k=1}^K \alpha_k$, where $\alpha_k = e_k + 1$, the predicted probability for class k is $p_k = \alpha_k/S$ and the prediction uncertainty u is calculated as $u = K/S$. EDL has been useful to detect data from unknown classes in prior literature (Bao et al., 2021; Zhao et al., 2023; Yu et al., 2024; Wang et al., 2024b; Peng et al., 2025). These literature motivates us to develop a EDL-based algorithm to detect novel deepfake categories. Compared with plug-in OSR techniques, EDL provides a more principled uncertainty estimation.

Challenges in applying EDL. In our approach, we employ EDL to collect evidence for face forgery detection. However, leveraging EDL to address the OSFFD problem meets the following challenges:

- 1) How to collect sufficient evidence in the OSFFD problem? Unlike conventional open set image classification, face forgery detection involves highly structured facial imagery. As a result, off-the-shelf EDL do not directly carry over to OSFFD with satisfactory performance. To bridge this gap, we extract evidential cues at two complementary levels: high-level semantic signals in the spatial domain and low-level artifacts in the frequency domain.
- 2) How can we achieve a comprehensive integration of collected complementary evidential cues? As both sources carry informative evidence, detection decisions should account for their joint contribution. The key challenge, therefore, is integrating the two independent uncertainty estimates into one well-calibrated and comprehensive metric. We address this issue by proposing a novel uncertainty-guided evidence fusion mechanism.

5 DUAL LEVEL EVIDENCE COLLECTION

Overview. To address the OSFFD problem, we propose the Dual-Level Evidential face forgery Detection (DLED) approach, which is exhibited in Figure 3. DLED exploits EDL through a dual-level evidential architecture that captures category characteristics of facial imagery across spatial and frequency domains, yielding sufficiently discriminative evidence. It addresses the evidence aggregation challenge with an uncertainty-guided fusion mechanism and further incorporates an uncertainty-improvement procedure to enhance the reliability of the resulting estimates. Together, these components enable DLED to detect novel fake categories by quantifying classification uncertainty across complementary levels and determining whether an existing prediction should be reassigned to the novel category.

270 **Spatial and Frequency Evidence.** Our DLED model addresses the evidence collection problem
 271 by extracting cues at two complementary levels: high-level spatial semantic signals and low-level
 272 frequency artifacts. Face forgeries generally fall into several common categories (FS, FR, EFS, and
 273 FE) based on their characteristics in the context of human visuals (Mirsky & Lee, 2021). We refer
 274 to these characteristics as deepfake category semantics, which is neglected by most existing works.
 275 Exploiting these semantics, the model can discern subtle differences among fake categories. To
 276 leverage both contextual and visual deepfake semantics, we employ the CLIP (Radford et al., 2021)
 277 architecture, a vision-language model designed to align image and text representations in a shared
 278 semantic space. Given an input image and the class textual descriptions, we then calculate the logit
 279 mass m_i for class i . In contrast to standard open set classification, relying solely on visual semantics
 280 fails to capture the structure of forgery images. We thus leverage low-level artifacts in the frequency
 281 domain as a complementary source of evidence. Specifically, for each input image, we obtain its
 282 frequency map by applying the Fast Fourier Transform and shifting the resulting spectrum to center
 283 the low-frequency components, thereby making them more prominent. To extract evidence from
 284 these complementary domains, we employ two parallel CLIP pipelines, each with a dedicated im-
 285 age encoder and text encoder. Since CLIP is not explicitly trained to capture forgery image patterns,
 286 particularly in the frequency domain, we adapt it by fine-tuning the encoders along with the text
 287 prompts while freezing all other pretrained parameters. For text prompts, we employ Context Opti-
 288 mization (Zhou et al., 2022), which augments class tokens with learnable prompt vectors to yield
 289 stronger context embeddings. For image and text encoders, we integrate LoRA (Hu et al., 2022)
 290 layers into them, which enhance the model’s understanding of deepfakes while not adding any addi-
 291 tional parameters during testing. Although we have two parallel branches for spatial and frequency
 292 level representations, we reduce memory consumption by sharing their pretrained parameters.
 293

294 **Evidential Uncertainty Estimation.** Our DLED model detects novel fake categories through ev-
 295 idential uncertainty estimation using Evidential Deep Learning (EDL) (Sensoy et al., 2018) in an
 296 end-to-end manner grounded in solid theoretical principles. EDL employs deep neural networks to
 297 output the parameters of a Dirichlet distribution over class probabilities, which is then used for both
 298 class prediction and uncertainty estimation. This process can be regarded as an evidence collection
 299 process. By leveraging EDL, our method quantifies the uncertainty associated with each prediction
 300 to assess its reliability. If the uncertainty is high, the model will reclassify the input as belonging to
 301 the novel class, thereby enabling the identification of faces from previously unseen fake categories.
 302

303 Specifically, for each of the spatial and frequency branches with classification logits mass m , our
 304 approach calculates the corresponding evidence $e = h(m)$ using an evidence function $h(\cdot)$ that
 305 guarantees e to be non-negative. During the training phase, to facilitate evidence collection, we
 306 independently apply the following EDL loss to each branch:
 307

$$\mathcal{L}_{EDL}(e, y) = \sum_{k=1}^K y_k (\log S - \log(e_k + 1)), \quad (4)$$

308 where $S = \sum_k \alpha_k$ and $\alpha_k = e_k + 1$, denoting the total strength of the Dirichlet distribution
 309 governed by $\{\alpha_1, \dots, \alpha_K\}$, and y is the one-hot K -class label. We also apply AvU regularization (Bao
 310 et al., 2021; Hammam et al., 2022) to each branch for uncertainty calibration. The EDL loss and
 311 AvU regularization minimize R_c and R_o in Eq. 3 separately.
 312

313 **Test-time Evidence Fusion.** To address the integration problem, we design a uncertainty-guided
 314 test-time evidence fusion mechanism. During model inference, according to EDL (Sensoy et al.,
 315 2018), the probabilities of different classes (belief masses) and the overall uncertainty mass can be
 316 calculated by $b_k = e_k / S$ and $u = K / S$. The K belief mass values and the uncertainty u are all
 317 non-negative and follow the sum-to-one rule: $\sum_{k=1}^K b_k + u = 1$. With this approach, we can get the
 318 belief and uncertainty for each branch.
 319

320 Our DLED model collects two independent sets of probability mass $M^s = \{\{b_k^s\}_{k=1}^K, u^s\}$ and
 321 $M^f = \{\{b_k^f\}_{k=1}^K, u^f\}$ from the spatial and frequency domains. Inspired by previous works (Han
 322 et al., 2020; 2022), we apply the Dempster’s combination rule (Sentz & Ferson, 2002) to get the
 323 joint detection probability mass set \tilde{M} in the following manner: $\tilde{M} = M^s \oplus M^f$. The specific
 324 calculation rules for belief mass and uncertainty mass are formulated as
 325

$$\tilde{b}_k = \gamma(b_k^s b_k^f + b_k^s u^f + b_k^f u^s), \quad \tilde{u} = \gamma u^s u^f, \quad (5)$$

324 where $\gamma = 1/(1 - \sum_{i \neq j} b_i^s b_j^f)$ is the scaling factor, normalizing the mass fusion to mitigate the
 325 effects of conflicting information between the spatial mass and frequency mass. With this newly
 326 obtained joint detection mass \widetilde{M} , the joint evidence and the parameters of the Dirichlet distribution
 327 are calculated as follows:
 328

$$329 \quad \widetilde{S} = \frac{K}{\widetilde{u}}, \quad \widetilde{e}_k = \widetilde{b}_k \times \widetilde{S}, \quad \text{and} \quad \widetilde{\alpha}_k = \widetilde{e}_k + 1. \quad (6)$$

331 For a test sample x^i , the model prediction \widetilde{p}_k^i for class k is computed as $\widetilde{p}_k^i = \widetilde{\alpha}_k^i / \widetilde{S}^i$.
 332

333 **Improved Uncertainty Estimation.** Considering $\widetilde{u} = K/\widetilde{S}$ and $\widetilde{S} = \sum_{k=1}^K (\widetilde{e}_k + 1)$, after dividing
 334 numerator and denominator by K , the uncertainty can be expressed as
 335

$$336 \quad \widetilde{u} = \frac{1}{1 + \frac{1}{K} \sum_1^K \{\widetilde{e}_1, \dots, K\}}, \quad (7)$$

338 which indicates that the uncertainty is assessed using the average evidence across all K classes.
 339 Therefore, when the input data shows high evidence from irrelevant classes, the estimated uncer-
 340 tainty will be overestimated resulting in a sub-optimal estimation. To solve this problem, we propose
 341 an improved uncertainty estimation by replacing the *average* evidence with *maximum* evidence:
 342

$$343 \quad \hat{u} = \frac{1}{1 + \max\{\widetilde{e}_1, \dots, K\}} = \frac{1}{\max\{\widetilde{\alpha}_1, \dots, K\}} \quad (8)$$

345 where $\{\widetilde{e}_1, \dots, K\}$ represents the set of K fused evidences. Our improved uncertainty measure offers
 346 the advantage of being less affected by low-evidence classes while retaining a normalized range be-
 347 tween 0 and 1 for better human understanding. Moreover, it directly reflects the model’s confidence
 348 in the predicted class. We recalculate the uncertainty \hat{u} with Eq. 8 after the evidence fusion to get
 349 better detection performance.

350 To determine if a face image belongs to an unseen fake category, our model compares its uncertainty
 351 \hat{u} with the uncertainty threshold for its predicted class. If the uncertainty falls above the threshold,
 352 the model reassigns the label to the novel category.

353 Table 1: Comparisons of model performance with diverse baseline methods implemented by ourselves for the
 354 OSFFD problem. We use different data configurations for the seen and unseen fake categories. For “FS”, “FR”,
 355 and “EFS”, we let each fake category be the unseen category and let the left two be seen categories. For “FE &
 356 SM”, we take FS, FR and EFS as seen categories and let FE and SM be the unseen categories. The best results
 357 are highlighted in **bold**.

Methods		FS		FR		EFS		FE & SM		Avg	
		Acc	DR	Acc	DR	Acc	DR	Acc	DR	Acc	DR
Two-stage	OC-FakeDect (Khalid & Woo, 2020) SBI (Shiohara & Yamasaki, 2022)	58.16 65.15	14.68 1.07	60.69 64.19	11.43 3.00	56.14 61.24	9.01 0.91	56.74 62.27	11.67 0.66	57.93 63.21	11.70 1.41
CNN-based + OSR	Xception (Rossler et al., 2019) SPSL (Liu et al., 2021) SIA (Sun et al., 2022) UCF (Yan et al., 2023a) NPR (Tian et al., 2024)	64.60 65.07 62.09 65.08 75.37	23.90 16.71 13.59 0.30 17.37	53.51 54.10 54.62 50.98 64.63	29.06 18.93 13.36 0.20 6.75	57.62 59.67 56.85 52.95 70.43	22.70 18.12 10.99 1.28 4.36	55.28 60.02 56.29 52.69 71.45	29.04 25.98 22.53 1.80 29.20	57.75 59.71 57.46 55.42 70.47	26.17 19.93 15.12 0.89 14.42
CLIP-based + OSR	CLIP Closed Set Finetuning CLIP Zero-Shot (Radford et al., 2021) UnivFD (Ojha et al., 2023) CLIPing (Khan & Dang-Nguyen, 2024) D^3 (Yang et al., 2025) Ours	67.24 52.30 68.81 66.44 70.46 71.37	\backslash 0.81 3.88 14.38 8.14 33.61	65.19 50.36 64.00 62.41 64.71 66.83	0.26 46.01 2.48 6.09 8.90 34.92	64.53 0.38 0.73 4.92 1.17 75.52	\backslash 47.62 63.21 61.29 61.65 34.71	66.24 0.25 66.34 66.26 66.33 74.48	\backslash 49.07 8.22 19.27 8.26 82.18	65.80 0.43 65.59 64.10 65.79 72.05	\backslash 3.83 11.16 6.62 46.35

368 6 EXPERIMENTS

371 **Datasets.** To evaluate model performance on the OSFFD problem, we conducted experiments using
 372 the comprehensive dataset DF40 (Yan et al., 2024b). DF40 collects fake faces from four distinct
 373 categories (“Face Swapping”, “Face Reenactment”, “Entire Face Synthesis”, and “Face Editing”) and
 374 includes a total of 40 diverse forgeries. Additionally, we introduced data from two “Stacked
 375 Manipulation” (SM) forgeries (He et al., 2021), in which techniques from multiple fake categories
 376 are applied within a single image. We treat these SM forgeries as an auxiliary fake category.

377 **Evaluation Protocols.** In OSFFD problem, the training set comprises real faces and fake faces from
 378 multiple known fake categories, while the test set additionally includes samples from unknown

378 fake categories. To evaluate the model’s performance, we first adopted the leave-one-out strategy in
 379 which one fake category from FS, FR, or EFS was withheld during training and treated as an unseen
 380 category during testing. Subsequently, all three fake categories (FS, FR, and EFS) were included as
 381 seen classes, and the model was evaluated on a test set containing additional forgeries from FE and
 382 SM, representing novel fake categories. As for the evaluation metric, we employed the multiclass
 383 classification Accuracy (**Acc**) and the Detection Rate (**DR**), where DR refers to the recall of the
 384 unseen fake categories.

385 We compared our DLED method with the following baseline methods. 1) Two-stage baselines: We
 386 introduced a second training stage for one-class out-of-distribution (OOD) detection methods: OC-
 387 FakeDetect (Khalid & Woo, 2020) and SBI (Shiohara & Yamasaki, 2022), in which an additional
 388 closed set multiclass model is independently trained to further classify the seen classes. For fair
 389 comparison, we used CLIP as the multiclass model’s backbone and finetuned it in the closed set
 390 manner with the cross-entropy loss; 2) CNN-based baselines: Xception (Rossler et al., 2019), SPSL
 391 (Liu et al., 2021), SIA (Sun et al., 2022), UCF (Yan et al., 2023a), and NPR (Tan et al., 2024);
 392 3) CLIP-based baselines: Zero-shot CLIP (Radford et al., 2021) and three established methods
 393 UnivFD (Ojha et al., 2023), CLIPing (Khan & Dang-Nguyen, 2024) and D^3 (Yang et al., 2025).

394 For the two-stage baselines, we let images recognized by the one-class model as seen classes go
 395 through the multiclass model to get their concrete class in testing. For the CNN-based and CLIP-
 396 based baselines, we replaced their binary classifier with a multi-class classifier trained in an end-to-
 397 end fashion and adopted the MaxLogit (Zhang & Xiang, 2023) technique in testing, because of its
 398 good performance in detecting unknown samples. For all algorithms that need a threshold to detect
 399 novel categories, we computed it from the training data such that 95% of the samples in each class
 400 are marked as known, which is the widely used setup in open set problems. Full implementation
 401 details are provided in the supplementary.

402 6.1 EVALUATION OF DETECTION PERFORMANCE

404 Open Set Face Forgery Detection.

406 Since the two-stage baselines rely on the closed
 407 set finetuned CLIP model as their multiclass clas-
 408 sifier, we also report the performance of this
 409 model independently. As shown in Table 1, most
 410 baseline models struggle to achieve high per-
 411 formance on both Accuracy (Acc) and Detection
 412 Rate (DR) simultaneously. Methods with higher
 413 Acc typically exhibit lower DR, and vice versa.
 414 It could also be observed that two-stage methods
 415 yield lower Acc than their base forgery classifier,
 416 indicating that OOD detectors and forgery classi-
 417 fiers are difficult to integrate in OSFFD with sat-
 418 isfactory performance. Besides, directly applying
 419 OSR techniques with an Xception backbone at-
 420 tains notably low Acc, underscoring that off-the-
 421 shelf OSR approaches are insufficient to solve the OSFFD problem. With more sophisticated designs
 422 tailored to face forgery detection, the baselines achieve higher Acc in most cases, confirming that
 423 efficient mechanisms for exploring forgery-specific representations are necessary to address OSFFD.

424 In comparison, our DLED model consistently achieves the highest DR across all scenarios and
 425 demonstrates superior average Acc, outperforming baseline methods in the majority of cases. These
 426 results highlight the effectiveness of DLED in discovering novel fake categories while maintaining
 427 strong recognition performance on real images and known fake categories.

428 **Real-vs-Fake Detection.** We also evaluate the proposed DLED model on the traditional Real-vs-
 429 Fake detection task, using the same data configuration as in the OSFFD problem. In this task, all
 430 baseline methods are implemented according to their original designs without modification. For
 431 our DLED model, any face predicted to belong to a fake category is classified as a fake sample.
 432 The results are shown in Table 2. It can be observed that DLED significantly outperforms these face
 433 forgery detection algorithms across all evaluation cases. These empirical results demonstrate that, in

Table 2: Comparisons of prediction accuracy with diverse baselines implemented by ourselves for the Real-vs-Fake detection task. Data configurations are the same as those in OSFFD. All baseline models are implemented following their original algorithms.

Methods	FS	FR	EFS	FE & SM	Avg
OC-FakeDect (Khalid & Woo, 2020)	48.09	48.45	48.18	47.16	47.97
SBI (Shiohara & Yamasaki, 2022)	50.13	50.36	50.07	49.96	50.13
Xception (Rossler et al., 2019)	71.73	67.98	67.19	67.49	68.60
SPSL (Liu et al., 2021)	72.29	65.87	70.34	69.57	69.52
SIA (Sun et al., 2022)	69.45	64.13	66.91	64.64	66.28
UCF (Yan et al., 2023a)	71.10	64.78	65.18	67.98	67.26
NPR (Tan et al., 2024)	80.76	75.73	77.67	77.21	77.84
CLIP Zero-Shot (Radford et al., 2021)	52.96	53.20	53.12	56.62	53.97
UnivFD (Ojha et al., 2023)	77.64	76.83	79.33	81.31	78.78
CLIPing (Khan & Dang-Nguyen, 2024)	78.46	77.15	79.58	81.09	79.07
D^3 (Yang et al., 2025)	78.56	77.00	79.67	79.81	78.76
Ours	87.22	85.93	83.52	84.97	85.41

addition to its strong performance on the OSFFD problem, the proposed DLED model also achieves competitive results on the traditional binary Real-vs-Fake deepfake detection task.

6.2 ABLATION STUDY

In this section, we conducted an ablation study on DLED. These experiments follow the same setup as described for OSFFD, and the results are summarized in Table 3.

Our results indicate that: 1) Compared to MaxLogit, EDL enhances model performance across both the spatial and frequency branches, indicating its superior capability in uncertainty estimation and, consequently, improved discovery of novel categories. 2) Although equipped with EDL, the pretrained CLIP model cannot be directly applied to the OSFFD problem in either the spatial or frequency domain, as indicated by its extremely poor performance (see the 2nd and 5th rows). Fine-tuning the prompts and integrating LoRA layers substantially improves the performance of both branches, highlighting the effectiveness of task-specific representation adaptation. 3) Without frequency information, the finetuned spatial branch with EDL exhibits an average performance drop of about 20% relative to the fused model (see the 3rd and 7th rows). This highlights the necessity of extracting complementary evidential cues across spatial and frequency domains to fully exploit forgery-specific signals and make more effective use of EDL, as well as the benefits of evidence integration. 4) By incorporating the improved uncertainty estimation, the full DLED model achieves the highest average Detection Rate, surpassing simple evidence fusion in most cases and thereby validating its effectiveness.

6.3 ANALYSIS OF EVIDENCE

To provide a clearer understanding of DLED’s behavior in OSFFD, we present visualizations of evidence distribution in Fig. 4. In this analysis, FR and EFS are treated as seen fake categories, while FS and FE represent novel categories.

Fig. 4 illustrates how uncertainty estimation facilitates the detection of novel fake categories among test samples. Each subfigure visualizes the Dirichlet distribution produced by DLED for the corresponding fake category. These visualizations demonstrate that the DLED model exhibits higher confidence when making predictions on seen classes, while showing greater prediction uncertainty for novel fake categories. This behavior enables DLED to effectively recognize newly emerging fake categories while simultaneously maintaining strong performance on known classes.

7 CONCLUSION

In this work, we reformulate the Open Set Face Forgery Detection (OSFFD) problem by removing the need for unlabeled novel data during model training, thereby enhancing its practicality for real-world applications. By treating the OSFFD as an uncertainty estimation problem, we proposed a novel algorithm, DLED, which effectively identifies unseen fake categories as novel while simultaneously classifying real and known fake categories. DLED leverages EDL to collect and fuse evidence from both spatial and frequency domains, exploiting category-specific semantics to estimate prediction uncertainty. Additionally, we propose an improved uncertainty formulation that enhances the model’s ability to detect novel fake categories. Extensive experiments under various testing configurations demonstrate that DLED substantially outperforms diverse baseline methods in addressing the OSFFD problem. Future work will focus on improving the efficiency of the proposed method and enabling rapid adaptation to the detected novel fake categories.

Table 3: Ablation Study of DLED. The table presents DR results under the same data configuration as used in the main OSFFD experiments.

Models	FS	FR	EFS	FE & SM	Avg
Spatial Branch	Zero-Shot with MaxLogit	0.81	0.26	0.38	0.25
	Zero-Shot with EDL	1.58	0.58	0.68	0.63
Frequency Branch	Finetuning with EDL	13.02	30.94	8.33	50.59
	Zero-Shot with MaxLogit	3.85	2.35	6.98	0.53
Two Branches	Zero-Shot with EDL	4.71	2.51	6.06	0.55
	Finetuning with EDL	14.34	8.49	7.69	90.36
Evidence Fusion		32.42	36.16	32.56	79.74
Full DLED		33.61	34.92	34.71	82.18
					46.36

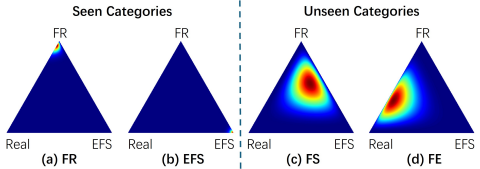


Figure 4: **Visualization of Evidence Distribution.** The evidence for seen fake categories FR and EFS is condensed in their corresponding corner with low uncertainty, while the evidence for novel fake categories FS and FE is sparse with higher uncertainty.

486 REFERENCES
487

488 Wentao Bao, Qi Yu, and Yu Kong. Evidential deep learning for open set action recognition. In
489 *Proceedings of the IEEE/CVF International Conference on Computer Vision*, pp. 13349–13358,
490 2021.

491 Junyi Cao, Chao Ma, Taiping Yao, Shen Chen, Shouhong Ding, and Xiaokang Yang. End-to-end
492 reconstruction-classification learning for face forgery detection. In *Proceedings of the IEEE/CVF*
493 *Conference on Computer Vision and Pattern Recognition*, pp. 4113–4122, 2022.

494

495 Guangyao Chen, Peixi Peng, Xiangqian Wang, and Yonghong Tian. Adversarial reciprocal points
496 learning for open set recognition. *IEEE Transactions on Pattern Analysis and Machine Intelli-*
497 *gence*, 44(11):8065–8081, 2021.

498 Michael Macedo Diniz and Anderson Rocha. Open-set deepfake detection to fight the unknown. In
499 *ICASSP 2024-2024 IEEE International Conference on Acoustics, Speech and Signal Processing*
500 (*ICASSP*), pp. 13091–13095. IEEE, 2024.

501

502 Lei Fan, Bo Liu, Haoxiang Li, Ying Wu, and Gang Hua. Flexible visual recognition by evidential
503 modeling of confusion and ignorance. In *2023 IEEE/CVF International Conference on Computer*
504 *Vision (ICCV)*, pp. 1338–1347, 2023. doi: 10.1109/ICCV51070.2023.00129.

505

506 Lei Fan, Mingfu Liang, Yunxuan Li, Gang Hua, and Ying Wu. Evidential active recognition: Intelli-
507 gent and prudent open-world embodied perception. In *Proceedings of the IEEE/CVF Conference*
508 *on Computer Vision and Pattern Recognition*, pp. 16351–16361, 2024.

509 Sharath Girish, Saksham Suri, Saketh Rambhatla, and Abhinav Shrivastava. Towards dis-
510 covery and attribution of open-world gan generated images. *2021 IEEE/CVF International*
511 *Conference on Computer Vision (ICCV)*, pp. 14074–14083, 2021. URL <https://api.semanticscholar.org/CorpusID:234357723>.

512

513 Qiqi Gu, Shen Chen, Taiping Yao, Yang Chen, Shouhong Ding, and Ran Yi. Exploiting fine-grained
514 face forgery clues via progressive enhancement learning. In *Proceedings of the AAAI Conference*
515 *on Artificial Intelligence*, volume 36, pp. 735–743, 2022.

516

517 Fabrizio Guillaro, Davide Cozzolino, Avneesh Sud, Nicholas Dufour, and Luisa Verdoliva. Trufor:
518 Leveraging all-round clues for trustworthy image forgery detection and localization. In *Proceed-*
519 *ings of the IEEE/CVF conference on computer vision and pattern recognition*, pp. 20606–20615,
520 2023.

521

522 Ahmed Hammam, Frank Bonarens, Seyed Eghbal Ghobadi, and Christoph Stiller. Predictive uncer-
523 tainty quantification of deep neural networks using dirichlet distributions. In *Proceedings of the*
524 *6th ACM Computer Science in Cars Symposium*, pp. 1–10, 2022.

525

526 Zongbo Han, Changqing Zhang, Huazhu Fu, and Joey Tianyi Zhou. Trusted multi-view classifica-
527 tion. In *International Conference on Learning Representations*, 2020.

528

529 Zongbo Han, Changqing Zhang, Huazhu Fu, and Joey Tianyi Zhou. Trusted multi-view classi-
530 fication with dynamic evidential fusion. *IEEE transactions on pattern analysis and machine*
531 *intelligence*, 45(2):2551–2566, 2022.

532

533 Yinan He, Bei Gan, Siyu Chen, Yichun Zhou, Guojun Yin, Luchuan Song, Lu Sheng, Jing Shao, and
534 Ziwei Liu. Forgerynet: A versatile benchmark for comprehensive forgery analysis. In *Proceed-*
535 *ings of the IEEE/CVF conference on computer vision and pattern recognition*, pp. 4360–4369,
536 2021.

537

538 Dan Hendrycks, Steven Basart, Mantas Mazeika, Andy Zou, Joe Kwon, Mohammadreza Mostajabi,
539 Jacob Steinhardt, and Dawn Song. Scaling out-of-distribution detection for real-world settings.
arXiv preprint arXiv:1911.11132, 2019.

540

541 Edward J Hu, Yelong Shen, Phillip Wallis, Zeyuan Allen-Zhu, Yuanzhi Li, Shean Wang, Lu Wang,
542 Weizhu Chen, et al. Lora: Low-rank adaptation of large language models. *ICLR*, 1(2):3, 2022.

540 Haojian Huang, Xiaozhennn Qiao, Zhuo Chen, Haodong Chen, Bingyu Li, Zhe Sun, Mulin Chen,
 541 and Xuelong Li. Crest: Cross-modal resonance through evidential deep learning for enhanced
 542 zero-shot learning. In *Proceedings of the 32nd ACM International Conference on Multimedia*,
 543 pp. 5181–5190, 2024.

544 He Huang, Nan Sun, Xufeng Lin, and Nour Moustafa. Towards generalized deepfake detection
 545 with continual learning on limited new data. In *2022 International Conference on Digital Image
 546 Computing: Techniques and Applications (DICTA)*, pp. 1–7. IEEE, 2022.

548 Ziheng Huang, Boheng Li, Yan Cai, Run Wang, Shangwei Guo, Liming Fang, Jing Chen, and
 549 Lina Wang. What can discriminator do? towards box-free ownership verification of generative
 550 adversarial networks. In *Proceedings of the IEEE/CVF international conference on computer
 551 vision*, pp. 5009–5019, 2023.

552 Audun Jøsang. *Subjective logic*, volume 3. Springer, 2016.

553

554 Tero Karras. Progressive growing of gans for improved quality, stability, and variation. *arXiv
 555 preprint arXiv:1710.10196*, 2017.

556 Hasam Khalid and Simon S Woo. Oc-fakedect: Classifying deepfakes using one-class variational
 557 autoencoder. In *Proceedings of the IEEE/CVF conference on computer vision and pattern recog-
 558 nition workshops*, pp. 656–657, 2020.

559

560 Sohail Ahmed Khan and Duc-Tien Dang-Nguyen. Clipping the deception: Adapting vision-
 561 language models for universal deepfake detection. In *Proceedings of the 2024 International
 562 Conference on Multimedia Retrieval*, pp. 1006–1015, 2024.

563 Iryna Korshunova, Wenzhe Shi, Joni Dambre, and Lucas Theis. Fast face-swap using convolutional
 564 neural networks. In *Proceedings of the IEEE international conference on computer vision*, pp.
 565 3677–3685, 2017.

566

567 Nico Lang, Vésteinn Snæbjarnarson, Elijah Cole, Oisin Mac Aodha, Christian Igel, and Serge Be-
 568 longie. From coarse to fine-grained open-set recognition. In *Proceedings of the IEEE/CVF con-
 569 ference on computer vision and pattern recognition*, pp. 17804–17814, 2024.

570 Nicolas Larue, Ngoc-Son Vu, Vitomir Struc, Peter Peer, and Vassilis Christophides. Seeable: Soft
 571 discrepancies and bounded contrastive learning for exposing deepfakes. In *Proceedings of the
 572 IEEE/CVF International Conference on Computer Vision*, pp. 21011–21021, 2023.

573

574 Ajian Liu, Shuai Xue, Jianwen Gan, Jun Wan, Yanyan Liang, Jiankang Deng, Sergio Escalera,
 575 and Zhen Lei. Cfpl-fas: Class free prompt learning for generalizable face anti-spoofing. In
 576 *Proceedings of the IEEE/CVF Conference on Computer Vision and Pattern Recognition*, pp. 222–
 577 232, 2024a.

578 Honggu Liu, Xiaodan Li, Wenbo Zhou, Yuefeng Chen, Yuan He, Hui Xue, Weiming Zhang, and
 579 Nenghai Yu. Spatial-phase shallow learning: rethinking face forgery detection in frequency do-
 580 main. In *Proceedings of the IEEE/CVF conference on computer vision and pattern recognition*,
 581 pp. 772–781, 2021.

582 Huan Liu, Zichang Tan, Chuangchuang Tan, Yunchao Wei, Jingdong Wang, and Yao Zhao. Forgery-
 583 aware adaptive transformer for generalizable synthetic image detection. In *Proceedings of the
 584 IEEE/CVF Conference on Computer Vision and Pattern Recognition*, pp. 10770–10780, 2024b.

585

586 Yuchen Luo, Yong Zhang, Junchi Yan, and Wei Liu. Generalizing face forgery detection with high-
 587 frequency features. In *Proceedings of the IEEE/CVF conference on computer vision and pattern
 588 recognition*, pp. 16317–16326, 2021.

589 Yisroel Mirsky and Wenke Lee. The creation and detection of deepfakes: A survey. *ACM computing
 590 surveys (CSUR)*, 54(1):1–41, 2021.

591

592 Aakash Varma Nadimpalli and Ajita Rattani. On improving cross-dataset generalization of deep-
 593 fake detectors. In *Proceedings of the IEEE/CVF Conference on Computer Vision and Pattern
 Recognition (CVPR) Workshops*, pp. 91–99, June 2022.

594 Yunsheng Ni, Depu Meng, Changqian Yu, Chengbin Quan, Dongchun Ren, and Youjian Zhao. Core:
 595 Consistent representation learning for face forgery detection. In *Proceedings of the IEEE/CVF*
 596 *conference on computer vision and pattern recognition*, pp. 12–21, 2022.

597 Yuval Nirkin, Yosi Keller, and Tal Hassner. Fsgan: Subject agnostic face swapping and reenactment.
 598 In *Proceedings of the IEEE/CVF international conference on computer vision*, pp. 7184–7193,
 599 2019.

600 Utkarsh Ojha, Yuheng Li, and Yong Jae Lee. Towards universal fake image detectors that generalize
 601 across generative models. In *Proceedings of the IEEE/CVF Conference on Computer Vision and*
 602 *Pattern Recognition*, pp. 24480–24489, 2023.

603 Kunyu Peng, Di Wen, Kailun Yang, Ao Luo, Yufan Chen, Jia Fu, M Saquib Sarfraz, Alina Roitberg,
 604 and Rainer Stiefelhagen. Advancing open-set domain generalization using evidential bi-level
 605 hardest domain scheduler. *Advances in Neural Information Processing Systems*, 37:85412–85440,
 606 2025.

607 Yuyang Qian, Guojun Yin, Lu Sheng, Zixuan Chen, and Jing Shao. Thinking in frequency: Face
 608 forgery detection by mining frequency-aware clues. In *European conference on computer vision*,
 609 pp. 86–103. Springer, 2020.

610 Alec Radford, Jong Wook Kim, Chris Hallacy, Aditya Ramesh, Gabriel Goh, Sandhini Agarwal,
 611 Girish Sastry, Amanda Askell, Pamela Mishkin, Jack Clark, et al. Learning transferable visual
 612 models from natural language supervision. In *International conference on machine learning*, pp.
 613 8748–8763. PMLR, 2021.

614 Andreas Rossler, Davide Cozzolino, Luisa Verdoliva, Christian Riess, Justus Thies, and Matthias
 615 Nießner. Faceforensics++: Learning to detect manipulated facial images. In *Proceedings of the*
 616 *IEEE/CVF international conference on computer vision*, pp. 1–11, 2019.

617 Walter J Scheirer, Anderson de Rezende Rocha, Archana Sapkota, and Terrance E Boult. Toward
 618 open set recognition. *IEEE transactions on pattern analysis and machine intelligence*, 35(7):
 619 1757–1772, 2012.

620 Murat Sensoy, Lance Kaplan, and Melih Kandemir. Evidential deep learning to quantify classifica-
 621 tion uncertainty. *Advances in neural information processing systems*, 31, 2018.

622 Murat Sensoy, Lance Kaplan, Federico Cerutti, and Maryam Saleki. Uncertainty-aware deep clas-
 623 sifiers using generative models. In *Proceedings of the AAAI conference on artificial intelligence*,
 624 volume 34, pp. 5620–5627, 2020.

625 Kari Sentz and Scott Ferson. Combination of evidence in dempster-shafer theory. 2002.

626 Wei Shen and Ruijie Liu. Learning residual images for face attribute manipulation. In *Proceedings*
 627 *of the IEEE conference on computer vision and pattern recognition*, pp. 4030–4038, 2017.

628 Weishi Shi, Xujiang Zhao, Feng Chen, and Qi Yu. Multifaceted uncertainty estimation for label-
 629 efficient deep learning. *Advances in neural information processing systems*, 33:17247–17257,
 630 2020.

631 Kaede Shiohara and Toshihiko Yamasaki. Detecting deepfakes with self-blended images. In *Pro-
 632 ceedings of the IEEE/CVF Conference on Computer Vision and Pattern Recognition*, pp. 18720–
 633 18729, 2022.

634 Aliaksandr Siarohin, Stéphane Lathuilière, Sergey Tulyakov, Elisa Ricci, and Nicu Sebe. First order
 635 motion model for image animation. *Advances in neural information processing systems*, 32, 2019.

636 Ke Sun, Hong Liu, Taiping Yao, Xiaoshuai Sun, Shen Chen, Shouhong Ding, and Rongrong Ji. An
 637 information theoretic approach for attention-driven face forgery detection. In *European Confer-
 638 ence on Computer Vision*, pp. 111–127. Springer, 2022.

639 Zhimin Sun, Shen Chen, Taiping Yao, Bangjie Yin, Ran Yi, Shouhong Ding, and Lizhuang Ma.
 640 Contrastive pseudo learning for open-world deepfake attribution. In *Proceedings of the IEEE/CVF*
 641 *International Conference on Computer Vision*, pp. 20882–20892, 2023.

648 Chuangchuang Tan, Yao Zhao, Shikui Wei, Guanghua Gu, Ping Liu, and Yunchao Wei. Rethinking
 649 the up-sampling operations in cnn-based generative network for generalizable deepfake detection.
 650 In *Proceedings of the IEEE/CVF Conference on Computer Vision and Pattern Recognition*, pp.
 651 28130–28139, 2024.

652 Haoqi Wang, Zhizhong Li, Litong Feng, and Wayne Zhang. Vim: Out-of-distribution with virtual-
 653 logit matching. In *Proceedings of the IEEE/CVF conference on computer vision and pattern*
 654 *recognition*, pp. 4921–4930, 2022.

655 Jun Wang, Omran Alamayreh, Benedetta Tondi, and Mauro Barni. Open set classification of gan-
 656 based image manipulations via a vit-based hybrid architecture. In *Proceedings of the IEEE/CVF*
 657 *Conference on Computer Vision and Pattern Recognition*, pp. 953–962, 2023a.

658 Jun Wang, Benedetta Tondi, and Mauro Barni. Bosc: A backdoor-based framework for open set
 659 synthetic image attribution. *arXiv preprint arXiv:2405.11491*, 2024a.

660 Ruofan Wang, Rui-Wei Zhao, Xiaobo Zhang, and Rui Feng. Towards evidential and class separa-
 661 ble open set object detection. In *Proceedings of the AAAI Conference on Artificial Intelligence*,
 662 volume 38, pp. 5572–5580, 2024b.

663 Sheng-Yu Wang, Oliver Wang, Richard Zhang, Andrew Owens, and Alexei A Efros. Cnn-generated
 664 images are surprisingly easy to spot... for now. In *Proceedings of the IEEE/CVF conference on*
 665 *computer vision and pattern recognition*, pp. 8695–8704, 2020.

666 Yezhen Wang, Bo Li, Tong Che, Kaiyang Zhou, Ziwei Liu, and Dongsheng Li. Energy-based
 667 open-world uncertainty modeling for confidence calibration. In *Proceedings of the IEEE/CVF*
 668 *International Conference on Computer Vision*, pp. 9302–9311, 2021.

669 Zhendong Wang, Jianmin Bao, Wengang Zhou, Weilun Wang, Hezhen Hu, Hong Chen, and
 670 Houqiang Li. Dire for diffusion-generated image detection. In *Proceedings of the IEEE/CVF*
 671 *International Conference on Computer Vision*, pp. 22445–22455, 2023b.

672 Mengjie Wu, Jingui Ma, Run Wang, Sidan Zhang, Ziyou Liang, Boheng Li, Chenhao Lin, Liming
 673 Fang, and Lina Wang. Traceevader: Making deepfakes more untraceable via evading the forgery
 674 model attribution. In *Proceedings of the AAAI Conference on Artificial Intelligence*, volume 38,
 675 pp. 19965–19973, 2024.

676 Zhiyuan Yan, Yong Zhang, Yanbo Fan, and Baoyuan Wu. Ucf: Uncovering common features for
 677 generalizable deepfake detection. In *Proceedings of the IEEE/CVF International Conference on*
 678 *Computer Vision*, pp. 22412–22423, 2023a.

679 Zhiyuan Yan, Yong Zhang, Xinhang Yuan, Siwei Lyu, and Baoyuan Wu. Deepfakebench: A com-
 680 prehensive benchmark of deepfake detection. *arXiv preprint arXiv:2307.01426*, 2023b.

681 Zhiyuan Yan, Yuhao Luo, Siwei Lyu, Qingshan Liu, and Baoyuan Wu. Transcending forgery speci-
 682 ficity with latent space augmentation for generalizable deepfake detection. In *Proceedings of the*
 683 *IEEE/CVF Conference on Computer Vision and Pattern Recognition*, pp. 8984–8994, 2024a.

684 Zhiyuan Yan, Taiping Yao, Shen Chen, Yandan Zhao, Xinghe Fu, Junwei Zhu, Donghao Luo,
 685 Chengjie Wang, Shouhong Ding, Yunsheng Wu, et al. Df40: Toward next-generation deepfake
 686 detection. *arXiv preprint arXiv:2406.13495*, 2024b.

687 Hong-Ming Yang, Xu-Yao Zhang, Fei Yin, Qing Yang, and Cheng-Lin Liu. Convolutional pro-
 688 totype network for open set recognition. *IEEE Transactions on Pattern Analysis and Machine*
 689 *Intelligence*, 44(5):2358–2370, 2020.

690 Tianyun Yang, Ziyao Huang, Juan Cao, Lei Li, and Xirong Li. Deepfake network architecture
 691 attribution. In *Proceedings of the AAAI Conference on Artificial Intelligence*, volume 36, pp.
 692 4662–4670, 2022.

693 Yongqi Yang, Zhihao Qian, Ye Zhu, Olga Russakovsky, and Yu Wu. D³: Scaling up deepfake
 694 detection by learning from discrepancy. In *Proceedings of the Computer Vision and Pattern*
 695 *Recognition Conference*, pp. 23850–23859, 2025.

702 Yang Yu, Danruo Deng, Furui Liu, Qi Dou, Yueming Jin, Guangyong Chen, and Pheng Ann Heng.
 703 Anedl: adaptive negative evidential deep learning for open-set semi-supervised learning. In *Pro-
 704 ceedings of the AAAI Conference on Artificial Intelligence*, volume 38, pp. 16587–16595, 2024.
 705

706 Hui Zhang and Henghui Ding. Prototypical matching and open set rejection for zero-shot semantic
 707 segmentation. In *Proceedings of the IEEE/CVF International Conference on Computer Vision*,
 708 pp. 6974–6983, 2021.

709 Xu Zhang, Svebor Karaman, and Shih-Fu Chang. Detecting and simulating artifacts in gan fake
 710 images. In *2019 IEEE international workshop on information forensics and security (WIFS)*, pp.
 711 1–6. IEEE, 2019.

712 Zihan Zhang and Xiang Xiang. Decoupling maxlogit for out-of-distribution detection. In *Proceed-
 713 ings of the IEEE/CVF Conference on Computer Vision and Pattern Recognition*, pp. 3388–3397,
 714 2023.

715 Chen Zhao, Dawei Du, Anthony Hoogs, and Christopher Funk. Open set action recognition via
 716 multi-label evidential learning. In *Proceedings of the IEEE/CVF Conference on Computer Vision
 717 and Pattern Recognition (CVPR)*, pp. 22982–22991, June 2023.

718 Haonan Zhong, Jiamin Chang, Ziyue Yang, Tingmin Wu, Pathum Chamikara Ma-
 719 hawaga Arachchige, Chehara Pathmabandu, and Minhui Xue. Copyright protection and account-
 720 ability of generative ai: Attack, watermarking and attribution. In *Companion Proceedings of the
 721 ACM Web Conference 2023*, pp. 94–98, 2023.

722 Kaiyang Zhou, Jingkang Yang, Chen Change Loy, and Ziwei Liu. Learning to prompt for vision-
 723 language models. *International Journal of Computer Vision*, 130(9):2337–2348, 2022.

724 Xinye Zhou, Hu Han, Shiguang Shan, and Xilin Chen. Fine-grained open-set deepfake detection
 725 via unsupervised domain adaptation. *IEEE Transactions on Information Forensics and Security*,
 726 2024.

727 Wanyi Zhuang, Qi Chu, Zhentao Tan, Qiankun Liu, Haojie Yuan, Changtao Miao, Zixiang Luo, and
 728 Nenghai Yu. Uia-vit: Unsupervised inconsistency-aware method based on vision transformer for
 729 face forgery detection. In *European conference on computer vision*, pp. 391–407. Springer, 2022.

730

731

732

733

734

735

736

737

738

739

740

741

742

743

744

745

746

747

748

749

750

751

752

753

754

755